Non-injection and low-temperature approach to colloidal photoluminescent PbS nanocrystals with narrow bandwidth

Liu, Tzu-Yu; Li, Minjie; Ouyang, Jianying; Zaman, Md. Badruz; Wang, Ruibing; Wu, Xiaohua; Yeh, Chen-Sheng; Lin, Quan; Yang, Bai; Yu, Kui

Publisher's version / Version de l'éditeur:
https://doi.org/10.1021/jp809171f
The journal of physical chemistry. C, Nanomaterials and interfaces, 113, 5, pp. 2301-2308, 2009-01-15

Non-Injection and Low-Temperature Approach to Colloidal Photoluminescent PbS Nanocrystals with Narrow Bandwidth

Tzu-Yu Liu,[†,§] Minjie Li,[†,||] Jianying Ouyang,[†] Md. Badruz Zaman,[†] Ruibing Wang,[†] Xiaohua Wu,[‡] Chen-Sheng Yeh,[§] Quan Lin,[||] Bai Yang,[||] and Kui Yu*[,†]

Steacie Institute for Molecular Sciences, National Research Council of Canada, Ottawa, Ontario K1A 0R6, Canada, Institute for Microstructural Sciences, National Research Council of Canada, Ottawa, Ontario K1A 0R6, Canada, Department of Chemistry, National Cheng Kung University, Tainan 701, Taiwan, and Key Laboratory for Supramolecular Structure and Materials, College of Chemistry, Jilin University, Changchun 130012, People's Republic of China

Received: October 16, 2008; Revised Manuscript Received: November 23, 2008

Colloidal photoluminescent (PL) PbS nanocrystals have attracted a lot of attention in various applications such as bioimaging and optical telecommunications due to their tunable bandgap in the near-infrared region of the electromagnetic spectrum. Hot-injection processes seem to be the best to engineer high-quality PbS nanocrystals. However, there is a limited body of literature documented on the syntheses, with little information on synthetic parameters affecting the optical properties of the product. Moreover, small PbS nanocrystals with large bandgap greater than 1.38 eV (ca. 900 nm) and narrow bandwidth are rarely reported, due to the fact that high-temperature growth in hot-injection processes leads to large nanocrystals rapidly. This manuscript deals with our noninjection and low temperature approach to small PbS nanocrystal ensembles with bandgap in wavelength shorter than 900 nm and with narrow bandwidth; the growth temperature can be as low as room temperature. For our noninjection approach, systematic study was performed on synthetic parameters affecting the growth, with the growth temperature in the range of 30−120 °C and octadecene (ODE) as a reaction medium. Different acids including oleic aicd (OA) were explored as surface ligands, while two lead source compounds, which are lead oxide (PbO) and lead acetate, and three S source compounds, which are bis(trimethylsilyl)sulfide ($(TMS)_2S$), thioacetamide (TAA), and elemental sulfur (S), were investigated. Generally, a solution of a lead precursor in ODE was first prepared via a reaction of a Pb-source compound and an acid; afterward, this solution was mixed with a S-source solution in ODE at room temperature. The use of $(TMS)_2S$ and OA bestows high-quality PbS nanocrystals, regarding narrow bandwidth of bandgap absorption and photoemission, without storage in dark for digestive and Ostwald ripening leading to self-focusing; in addition to the various acids and Pb and S source compounds explored, feed molar ratios of acid-to-Pb and Pb-to-S, as well as reactant concentrations were thoroughly investigated. Low acid-to-Pb and high Pb-to-S feed molar ratios together with high-reactant concentrations favor the formation of small PbS nanocrystals; meanwhile, from one synthetic batch, the growth of PbS nanocrystals in size is tunable mainly via temperature in addition to growth periods. The PbS nanocrystals exhibit bandwidth (full width at half-maximum) as narrow as ca. 100 nm with growth temperature of 70 °C. Thus, our noninjection approach features easy handling with high reproducibility and high-quality PbS nanocrystals with large bandgap but narrow bandwidth. Finally, bandgap engineering of our as-synthesized PbS nanocrystals was performed straightforwardly at room temperature via the mixing of a solution of Cd oleate in ODE; significant blueshift of bandgap absorption and photoemission with enhanced PL efficiency was accomplished.

1. Introduction

Colloidal semiconductor quantum dots (QDs) have been attracting enormous interest due to their tunable optical properties via the control of size, structure, and composition.[1−4] The quantum confinement effects become operative when the particle diameter is less than or comparable to that of a photogenerated exciton in corresponding bulk materials. Among II−VI, III−V, and IV−VI semiconductor nanocrystals, PbS and PbSe are particularly interesting. With large exciton Bohr radii of 20 nm (for PbS) and 46 nm (for PbSe),[5] both charge carriers, which are electron and hole, contribute almost equally to the exciton Bohr radii, leading to enhanced confinement of the both carriers. With the confinement energy splits about equally between the two carriers, PbS and PbSe QDs exhibit strong size-dependent properties and simple electron spectra.[5] With similar quantum confinement, the surface of the IV−VI nanocrystals contributes relatively little compared to that of the II−VI and III−V QDs.[5] Meanwhile, with a small bulk bandgap of 0.41 eV, the bandgap of PbS QDs can be engineered in the range of 600−900 nm to create potential in the applications aiming at bio-oriented and energy-related areas.[4]

To meet these potentials, high-quality PbS QD ensembles with small size distribution for narrow bandwidth (full width

* To whom correspondence should be addressed. E-mail: kui.yu@nrc.ca.
† Steacie Institute for Molecular Sciences, National Research Council of Canada.
§ National Cheng Kung University.
|| Jilin University.
‡ Institute for Microstructural Sciences, National Research Council of Canada.

10.1021/jp809171f CCC: $40.75
Published on Web 01/15/2009

at half-maximum, fwhm) of absorption and emission, good stability, and reasonable quantum yield are in demand. Among the significant efforts made on synthesizing II−VI, III−V, and IV−VI semiconductor materials, there is a limited body of literature on the synthesis of PbS QDs.[6,7] Furthermore, most of the synthetic efforts reported on PbS nanomaterials target large size with different morphologies, including flower-shaped, dendritic-shaped, hexapodlike, wirelike, tubular, and hollow materials,[8−13] leaving the synthesis of small PbS QDs with bandgap in the range of 600−900 nm still challenging.

A few synthetic approaches to spherical PbS nanocrystals have been carried out, including colloidal chemistry,[14−17] growth in polymer,[18] electrochemical preparation,[19] and electron beam irradiation.[20] For water-soluble PbS nanocrystals, lead acetate and sodium sulfide were used as reactant sources, while thioglycerol and dithioglycerol as capping agents in water; with different Pb-to-S feed molar ratios, the resulting PbS nanocrystals exhibited emission in the range of 1000−1400 nm.[14] For non-water-soluble colloidal PbS QDs, the hot-injection approach reported by Hines and Scholes seems to be the best to engineer high-quality QD ensembles.[15a] This hot-injection method was conducted by heating a mixture of lead oxide (PbO) and oleic acid (OA, as capping ligands) in octadecene (ODE) at 150 °C under Ar for one hour followed by the injection of a solution of $(TMS)_2S$ (sulfur source) in ODE at 150 °C. After the hot injection, the growth was kept either at 80−140 °C or room temperature. It was declared that the growth temperature lower than 150 °C was preferred in order to separate the nucleation and growth for the absence of rapid defocusing of the size distribution. The resulting PbS QDs exhibited bandgap absorption ranging from 800 to 1800 nm. However, little information was reported on the growth temperature and periods affecting the bandgap of the resulting nanocrystals, or on the bandwidth of the as-synthesized nanocrystals; namely, it is not clear that the optical spectra reported were from the as-synthesized nanocrystals or from dark-stored ripened ones experienced self-focusing. With lead acetate and H_2S gas as reactant sources, OA as capping agent, and *n*-decane as a reaction medium, PbS nanocrystals with absorption peaking in the range of 580−900 nm and photoemission of 770−1000 nm were reported. After the addition of H_2S at 40−130 °C, the growth period was as short as seconds; such a request on the short growth period is due to the rapid reaction between lead oleate and H_2S. Accordingly, each synthetic batch only produced one ensemble.[15b] Also, no detailed study was reported on the synthetic parameters such as acid-to-Pb and Pb-to-S feed molar ratios affecting the bandgap of the resulting PbS QDs.

We report in this manuscript our low-temperature and noninjection one-pot approach to high-quality colloidal photoluminescent (PL) PbS QDs with narrow bandwidth and bandgap in the range of 600−900 nm. This ready synthesis was carried out in ODE as a reaction medium, with the growth temperature as low as room temperature to 120 °C. The growth kinetics was monitored by the temporal evolution of the optical properties of the resulting QDs. We explored the nature of lead source compounds, the nature of acids as surface ligands, and different S source compounds, with the optimal of PbO, OA, and $(TMS)_2S$, respectively. Also, we investigated in detail other synthetic parameters affecting the formation of the PbS nanocrystals, including acid-to-Pb and Pb-to-S feed molar ratios, reactant concentrations, and growth temperature. Various PbS nanocrystal ensembles of different sizes can be engineered from one synthetic batch; mainly, it is the growth temperature rather than growth period that controls the nanocrystal size. Accordingly, this noninjection synthesis features easy handling with high reproducibility. Furthermore, we address shelf-storage stability in dilute dispersion and in reaction medium at room temperature under room light; it is surprising that these small PbS QDs are fairly stable when stored in their reaction medium. Finally, we present bandgap engineering of as-synthesized PbS QDs via the postsynthesis treatment of a solution of Cd oleate in ODE at room temperature; significant blueshift of bandgap absorption and photoemission together with enhanced PL efficiency was achieved.

2. Experimental Section

2.1. Synthesis of PbS Nanocrystals. Typically, two solutions were prepared. For the preparation of a Pb-precursor solution, 0.09 g (0.4 mmol) of PbO (Aldrich, 99.999%), 0.25 mL (0.8 mmol) of OA (Aldrich, tech., 90%), and 3.75 mL of ODE (Aldrich, tech., 90%) were loaded in a 100-mL three-neck reaction flask at room temperature; afterward, the reaction flask was degassed at room temperature for 30 min and was heated up to 120 °C for one hour under vacuum to form the precursor of lead oleate. Subsequently, the reaction flask was switched to N_2 and cooled down to room temperature. For the preparation of a S-precursor solution, 2 mL of ODE was degassed for one hour under vacuum; afterward, 42 μL (0.2 mmol) of $(TMS)_2S$ (Fluka) was added under the protection of N_2. This resulting S-source solution in ODE was stirred for 10 min and mixed into the reaction flask consisting of the Pb-precursor solution with a syringe. Therefore, this typical synthesis is with 4OA-to-2Pb-to-1S feed molar ratios and the $(TMS)_2S$ concentration of 0.035 M.

After the mixing of the S solution into the Pb solution, the growth was carried out at either room temperature or elevated temperature. For the latter, the reaction flask was heated up by a rate of ca. 2 °C/min with aliquots taken at room temperature, 40, 50, 60, 70, 80, 90, 100 110, and 120 °C; usually, it took about 45 min to reach 120 °C. Each aliquot sampled was kept in a vial and cooled down immediately in a water bath at room temperature. A specified amount of each sample (30 μL) was dispersed into 3 mL of toluene (ACP, 99.50%) for the measurement of the optical properties of the growing nanocrystal ensemble. Absorption spectra were collected on a Cary 5000 UV/vis/NIR spectrometer using a 1-nm data collection interval and scan rate of 600nm/min, while photoemission experiments were performed on a Fluoromax-3 spectrometer (Jobin Yvon Horiba, Instruments SA), with a 450-W Xe lamp as the excitation source, an excitation wavelength of 500 nm (if not specified), an increment of data collection of 2 nm, and the slits for excitation and emission of 3 nm.

2.1.1. Various Pb and S Source Compounds Studied. Two Pb and three S source compounds were studied; they were PbO (Aldrich, 99.999%) and lead acetate trihydrate ($PbAc_2 \cdot 3H_2O$, Anachemia, 99.0−103.0%), and $(TMS)_2S$ (Fluka), thioacetamide (TAA, Sigma-Aldrich, 99+%), and elemental sulfur (Anachemia, precipitated). Elemental S was used together with 2,2′-dithiobisbenzothiazole (MBTS, Aldrich, 99%).[6f]

2.1.2. Various Acid-to-Pb and Pb-to-S Feed Molar Ratios and Reactant Concentrations. For the typical synthesis of the PbS QDs mentioned above, we investigated the effect of (a) OA-to-PbO feed molar ratios including 4OA-2Pb-1S, 8OA-2Pb-1S, 16OA-2Pb-1S, and 32OA-2Pb-1S, (b) PbO-to-$(TMS)_2S$ feed molar ratios including 4OA-2Pb-1S, 8OA-4Pb-1S, and 16OA-8Pb-1S, and (c) S concentrations with a fixed OA-to-PbO-to-$(TMS)_2S$ feed molar ratio of 8OA-4Pb-1S. Table 1 summarizes in detail the synthetic conditions of the reactions performed.

TABLE 1: Systematic Study of the Non-Hot-Injection to Colloidal PL PbS Quantum Dots with OA and PbO in 3.75 mL of ODE and $(TMS)_2S$ in 2 mL of ODE

OA-to-Pb-to-S (molar ratios)	OA (mmol)	PbO (g)	(TMS)2S (uL)
(a) OA-to-PbO Feed Molar Ratios			
4:2:1	0.8	0.09	42
8:2:1	1.6	0.09	42
16:2:1	3.2	0.09	42
32:2:1	6.4	0.09	42
(b) PbO-to-$(TMS)_2S$ Feed Molar Ratios			
4:2:1	0.8	0.09	42
8:4:1	1.6	0.18	42
16:8:1	3.2	0.36	42
(c) S Concentrations			
4:2:0.5	0.4	0.05	10
8:4:1	0.8	0.09	21
16:8:2	1.6	0.18	42

2.1.3. Various Capping Ligands Used. Fatty acids with various carbon-chain lengths from C8−C24 were investigated; they were octanoic acid (C8, Sigma, 99%), dodecanoic acid (C12, Sigma, 99%), myristic acid (C14, Sigma, 99−100%), stearic acid (C18, Fluka, purity ~98.5%), and lignoceric acid (C24, Aldrich 99%). The study was performed with one of the acids replacing oleic acid in the typical synthesis recipe. During the cooling process, which was after the formation of a Pb precursor at 120 °C and before the addition of the $(TMS)_2S$ solution at room temperature, it was noticed that all of the Pb precursors, namely, Pb-acid complexes, precipitated out even when the temperature was 80 °C during the cooling from 120 °C to room temperature.

2.2. Storage Stability of As-Synthesized PbS Nanocrystals and Further Bandgap Engineering. The shelf-storage stability of the resulting PbS QDs was explored. The PbS ensemble sampled at 70 °C from the typical synthesis batch with the 4OA-to-2Pb-to-1S feed molar ratios was kept in a vial while stored on benchtop at room temperature under domestic light for days; meanwhile, 30 μL of this ensemble was dispersed in 3 mL of toluene and kept under the same conditions for days. The storage stability was monitored with optical measurements.

To further engineer the bandgap of the PbS QDs, CdS coating was conducted under nitrogen at room temperature by adding preprepared Cd oleate to as-synthesized PbS QDs. The Cd oleate was prepared with the reaction of 0.0514 g (0.4 mmol) of CdO (Aldrich 99%) and 0.375 mL (1.2 mmol) of OA in 3.625 g of ODE at 180−190 °C under nitrogen for 2 h and then cooled to room temperature under nitrogen.

2.3. Purification for X-ray Diffraction (XRD) and Transmission Electron Microscopy (TEM). A mixture of methanol and acetone (with a 1-to-2 volume ratio) was dropwise added into as-synthesized PbS QDs to precipitate the nanocrystals. After centrifugation (4000 rpm for 10 min), the supernatant was decanted, and toluene was added to disperse the PbS QDs with shaking. Such a process of the purification was carried out three times. For TEM characterization, a purified sample stored in toluene was deposited on a carbon-coated copper grid and was studied on a JEOL JEM-2100F electron microscope operating at 200 kV and equipped with a Gatan UltraScan 1000 CCD camera. Powder XRD patterns were recorded at room temperature on a Bruker Axs D8 X-ray diffractometer using Cu Kα radiation in a $\theta-\theta$ mode. The generator was operated at 40 kV and 40 mA, and data were collected between 5 and 80° in 2θ with a step size of 0.1° and a counting time of 5 s per step. XRD samples were prepared by depositing the purified nanocrystals on low-background quartz plates.

3. Results and Discussion

This manuscript addresses our noninjection and low-temperature approach to colloidal PL PbS QDs in ODE; thus, the results and discussion consist of two parts. The synthesis of the PbS QDs is mainly presented in section 3.1, while the storage stability of the resulting PbS QDs and further bandgap engineering are dealt with in section 3.2. The comparison of hot-injection and noninjection approaches on the control of the size of the resulting PbS QDs is discussed in Figure S1 of the Supporting Information. In section 3.1, various synthetic parameters affecting the quality of the PbS QDs are presented in detail, in a sequence of sulfur and lead source compounds (section 3.1.1), OA-to-PbO feed molar ratios (section 3.1.2a), PbO-to-$(TMS)_2S$ feed molar ratios (section 3.1.2b), feed concentrations (section 3.1.2c), and various acids as capping ligands (Session 3.1.3.).

3.1. Noninjection Approach to Colloidal PL PbS Nanocrystals. Figure 1 shows the temporal evolution of the optical properties of the growing nanocrystals from three synthetic batches with the typical synthesis recipe of the 4OA-2PbO-1$(TMS)_2S$ feed molar ratios. After the mixing of the two Pb-precursor and S-precursor solutions at room temperature, the color of the resulting solution changed from clear yellow to pink, red, and then brown, indicating the presence of a nucleation/growth process of PbS nanocrystals. Figure 1A shows the temporal evolution of the optical properties of the growing nanocrystals with the growth temperature kept at room temperature (30 °C), while Figure 1B shows the same at 40 °C. During the growth periods monitored up to 4 h, the first excitonic absorption peaks and emission peaks exhibit relatively small redshifts for the nanocrystals from the batch with 30 °C growth, as compared to those from the batch with 40 °C growth. Part C in Figure 1 shows the temporal evolution of the absorption of the growing nanocrystals from the batch with its reaction temperature increased from room temperature (30 °C) to 120 °C at a rate of ca. 2 °C/min. During such a temperature increase, the resulting PbS nanocrystals exhibit bandgap absorption with a redshift from ca. 633 nm to ca. 859 nm; such redshift indicates significant growth in size of the PbS QDs as temperature increases. Moreover, each QD ensemble sampled at the different temperature exhibits a single absorption peak with a high symmetry which suggests narrow size distribution (during the whole range investigated of the growth temperature). Careful examination recommends the presence of the decrease of size distribution takes place up to 70−80 °C from the decrease of the bandwidth of the PbS nanocrystal ensembles. The emission spectrum of the 70 °C growth PbS QDs is shown in the inset of Figure 1C, whose bandgap absorption and emission peak at 712 and 822 nm, respectively. Clearly, the bandwidth is narrow, with full width at half-maximum (fwhm) on the order of ca. 100 nm. It is worthy to notice that this fwhm value is small, to the best of our knowledge, and comparable to the best reported with other synthetic approaches.[14−17] Also, the quantum yield of the 70 °C growth PbS QDs in toluene was estimated to be of the order of 20% (relative to R590 in ethanol). It is necessary to point out that the PL fwhm of a single PbS dot emitting at ca. 790 nm was reported to be ca. 50 nm;[21] the large homogeneous broadening was argued to be related to enhanced acoustic phonon coupling.[22]

Figure 2 shows the powder XRD patterns of the 70 °C growth PbS QDs (shown in Figure 1C-e) (top) and bulk cubic rocksalt PbS (bottom). The XRD patterns indicate that the PbS QDs have a cubic rocksalt structure. It is clear that the diffraction peaks in the top part of Figure 2 are broader than those in the bottom part of Figure 2 due to the smaller QD size. The QD

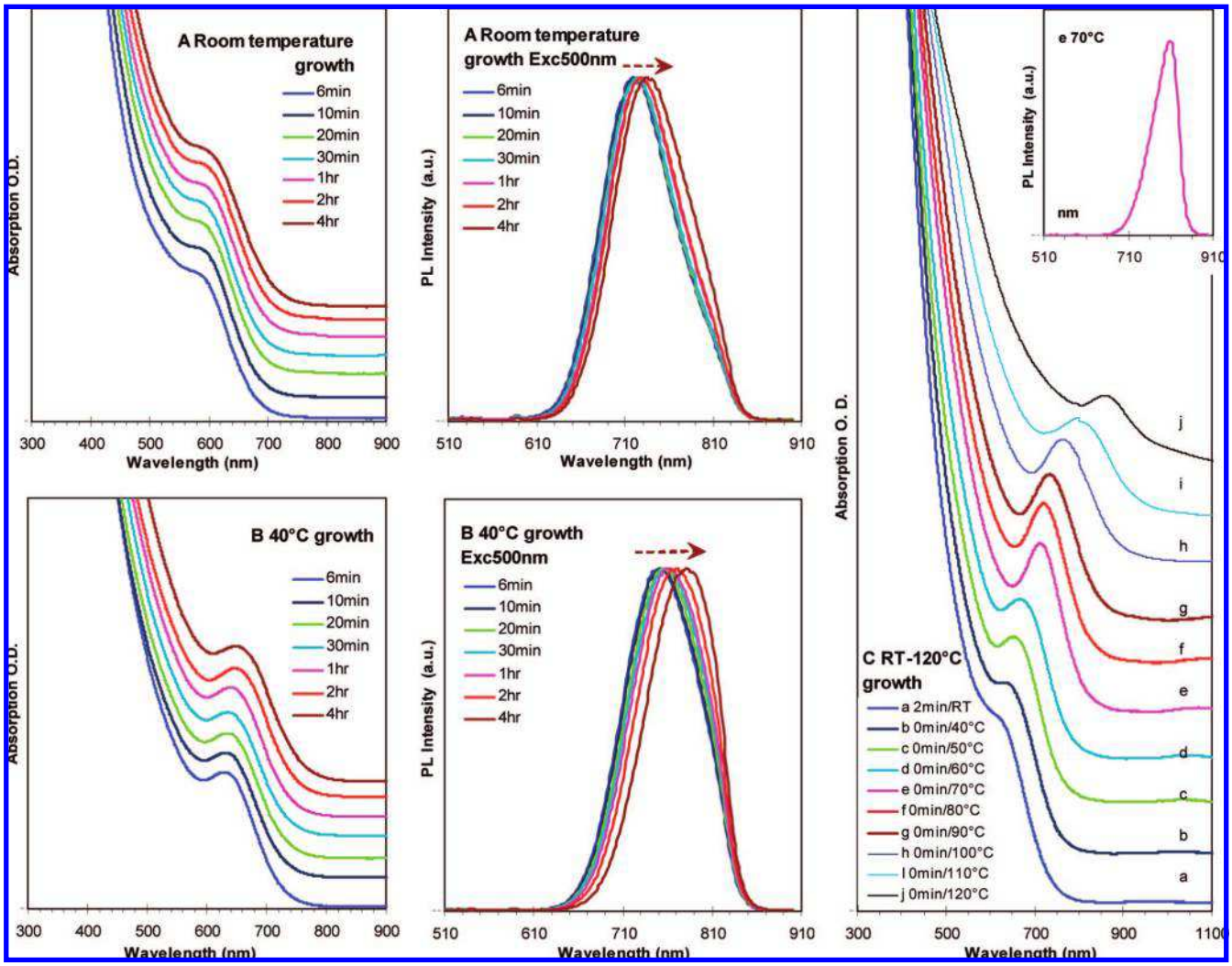

Figure 1. Temporal evolution of the optical properties of PbS QDs from three synthetic batches with the same recipe of 4OA-to-2PbO-to-1$(TMS)_2S$ feed molar ratios (Table 1). Nanocrystals with room temperature growth (ca. 30 °C) (A), 40 °C growth (B), and room temperature to 120 °C growth (C). The nanocrystals were dispersed in toluene for the absorption and emission (with excitation wavelength of 500 nm) measurements.

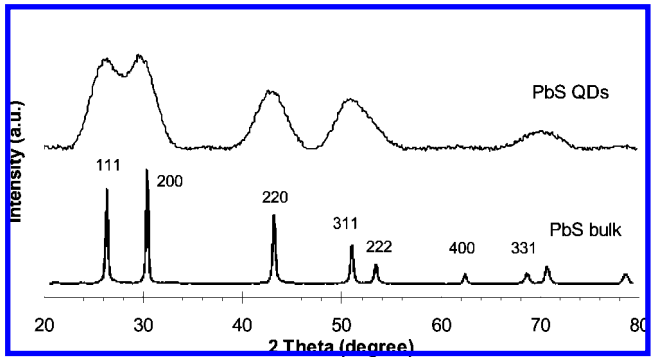

Figure 2. Powder XRD patterns of the 70 °C growth PbS QDs (shown in Figure 1C-e with absorption peaking at ca. 712 nm) (top) and of bulk cubic rock salt PbS (bottom). The diffraction peaks are indexed.

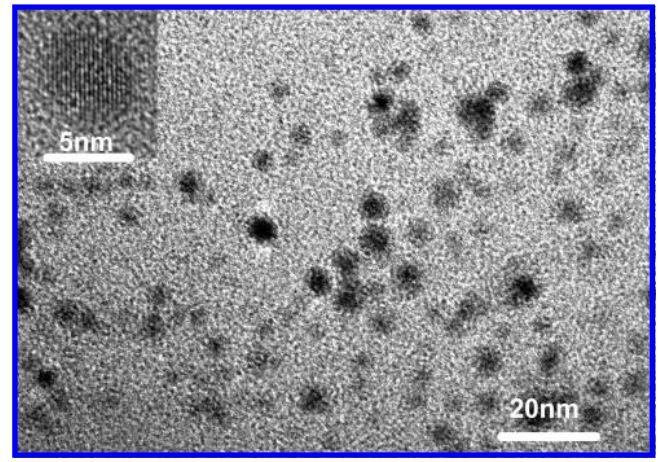

Figure 3. A typical TEM image of the 50 °C growth PbS nanocrystals (shown in Figure 1C-c, whose absorption peaking at 651 nm); the inset shows a high-resolution TEM image of the same.

size is estimated to be ~2.59 nm by the Scherrer equation with the fwhm of the diffraction peak (220).

Figure 3 shows a typical TEM image of the 50 °C growth PbS QD ensemble with bandgap absorption at ca. 651 nm (shown in Figure 1C-c); the TEM image demonstrates that the size distribution is narrow. The insert is one corresponding high-resolution TEM image showing the crystal fringes with the scale bar of 5 nm. It has been acknowledged that different characterization tools such as XRD, TEM, and Raman scattering, etc., give slightly different results in determining the QD sizes.[6]

Let us turn our attention to the comparison of noninjection and hot-injection approaches to synthesize PbS nanocrystals.

Our noninjection approach features relatively mild synthetic conditions with high reproducibility and large-scale capability, as compared to the existing hot-injection approach,[15a] leading to relatively small-sized PbS nanocrystals particularly at low growth temperature. It is noteworthy that the bandgap absorption peak positions of our PbS nanocrystals (shown in Figure 1) located at relatively short wavelengths compared to those reported by the hot-injection approach;[15a] moreover, various nanocrystal ensembles, which are different in sizes, can be engineered from one synthetic batch. Especially, the as-synthesized nanocrystal ensembles exhibit narrow bandwidth; no dark storage is needed for digestive and Oswald ripening leading to self-focusing, while postannealing in dark was usually necessary for the nanocrystals reported before.[14,15a] Parallel experiments with both noninjection and hot-injection methods were carried out with the same recipe, as shown in Figure S1 of Supporting Information. With the 4OA-2PbO-1$(TMS)_2S$ syntheses, the 100 °C growth PbS nanocrystals exhibit bandgap absorption peaking at ca. 762 nm with our noninjection approach (Figure 1C-h) and at ca. 1009 nm with our hot-injection approach (injection temperature 150 °C) (left panel of Figure S1 of Supporting Information). With 16OA-2PbO-1$(TMS)_2S$ syntheses, the 70 °C growth PbS nanocrystals exhibit bandgap absorption peaking at ca. 913 nm with our noninjection approach and at ca. 987 nm with our hot-injection approach (injection temperature 70 °C) (right panel of Figure S1 of Supporting Information). It is obvious that from one synthetic batch the noninjection approach leads to ready size control via raising temperature, namely the growth of particles can be easily facilitated with temperature increase, while the hot-injection approach does not but with the size controlled mainly by the injection temperature.

To achieve the optimal synthetic condition shown in Figure 1, we studied various synthetic parameters, including sulfur and lead source compounds, OA-to-PbO feed molar ratios, PbO-to-$(TMS)_2S$ feed molar ratios, feed concentrations, and various acids as capping ligands.

3.1.1. Various Sulfur and Lead Source Compounds Explored. Three sulfur sources, bis(trimethylsilyl)sulfide ($(TMS)_2S$), TAA, and elemental S were investigated to synthesize PL PbS QDs. TAA has often been used to synthesize PbS nanocrystals with various morphologies in aqueous media.[9,23,24] With elemental S as the S source, 2,2-dithiobis(benzothiazole) (MBTS) was used together to enhance S reactivity.[6f] With the typical synthesis recipe but the different S sources, three batches under the same reaction condition of the 4OA-to-2PbO-to-1S feed molar ratios were monitored, with the growth temperature increasing from room temperature up to 240 °C. The temporal evolution of the optical properties (Figure S2 of Supporting Information) reveals that these three S source compounds have different reactivity and decrease in the order $(TMS)_2S$, TAA, elemental S. The formation of PbS nanocrystals started at room temperature with $(TMS)_2S$, ca. 40 °C with TAA, and ca. 180 °C with elemental S. The optimal growth temperature is in the range of 30−120 °C with $(TMS)_2S$ and 60−100 °C with TAA, which results in QDs with good absorption with narrow bandwidth similar to that obtained with $(TMS)_2S$; however, the resulting PbS QDs exhibit poor PL. With elemental S, when the temperature is higher than 180 °C, PbS QDs with very broad absorption were obtained with no PL at all; meanwhile, large particles precipitated out.

Two Pb source compounds were also compared; they are PbO and $PbAc_2$. With the typical synthesis recipe but the different Pb sources, two batches under the otherwise same reaction conditions of the 4OA-to-2Pb-to-1$(TMS)_2S$ feed molar ratios were monitored, while their reaction temperature increased from room temperature up to 120 °C. When the growth temperature is below 90 °C, the PbS nanocrystals synthesized from the two batches are similar in size, as suggested by the similarity in peak positions of absorption and photoemission monitored; (the absorption spectra are shown in Figure S3 of Supporting Information). Careful comparison of the peak position leads to the argument that the use of $PbAc_2$ gives slightly faster rate of nucleation/growth. When the growth temperature is above 90 °C, such difference becomes pronounced, namely, the $PbAc_2$−PbS nanocrystals started to grow faster, which might be the consequence of the existence of acetate and acetic acid. A similar phenomenon was observed in the synthesis of PbSe nanocrystals and was interpreted as the presence of both acetate and oleate ligands at the Pb sites on the dot surface;[25] it is easy to understand that elevated temperature facilitated molecular mobility and the presence of small acetate ligands led to large nanocrystals.[25]

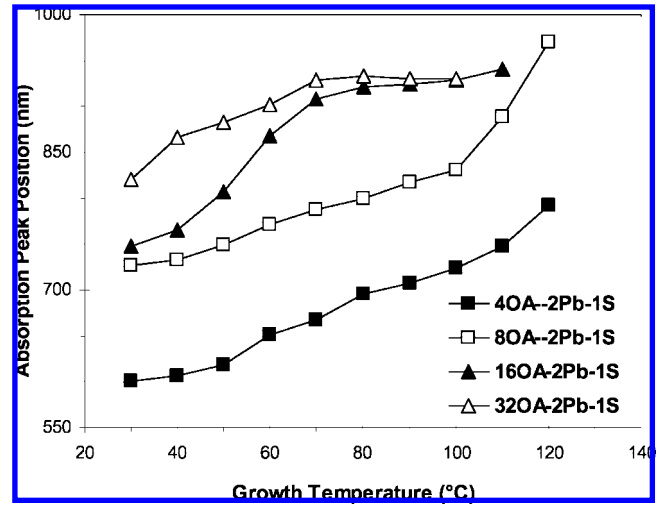

Figure 4. Comparison of the acid-to-Pb feed molar ratios affecting the growth of PbS QDs with a fixed Pb-to-S feed molar ratio and S concentration under the synthetic conditions given in Table 1a. The absorption peak positions are presented by *y* axis in nanometers, while the growth temperature is seen on the *x* axis. The studied feed molar ratios are 4OA-2Pb-1S (■), 8OA-2Pb-1S (□), 16OA-2Pb-1S (▲), and 32OA-2Pb-1S (Δ).

3.1.1.a. Effect of OA-to-PbO Feed Molar Ratios with a 2PbO-to-1$(TMS)_2S$ Fixed Feed Molar Ratio at 0.035 M Concentration of $(TMS)_2S$. With the typical synthetic condition, OA-to-PbO-to-$(TMS)_2S$ feed molar ratios of 4OA-2Pb-1S, 8OA-2Pb-1S, 16OA-2Pb-1S, and 32OA-2Pb-1S were investigated. Figure 4 shows the absorption peak positions of the resulting PbS nanocrystals at different growth temperatures from the four synthetic batches; the absorption spectra are presented in Figure S4 of Supporting Information. When the OA-to-PbO feed molar ratio was smaller than 2:1, PbO was not able to dissolve completely in the form of lead oleate in ODE. Among the four acid-to-Pb feed molar ratios studied in Figure 4, (4−8)OA-to-2Pb is preferred to synthesize PbS QD ensembles with narrow size distribution and tunable sizes from one synthetic batch. Careful comparison distinguishes two growth stages during the increase of the temperature, before and after 70 °C: before 70 °C, batches with larger acid-to-Pb feed molar ratios gave larger nanocrystals; after 70 °C, little difference in size between the 32OA-2Pb-1S and 16OA-2Pb-1S batches was observed; in addition, significant broadening was noticed for 32OA-2Pb-1S at 100 °C, 16OA-2Pb-1S at 110 °C, and 8OA-2Pb-1S at 120

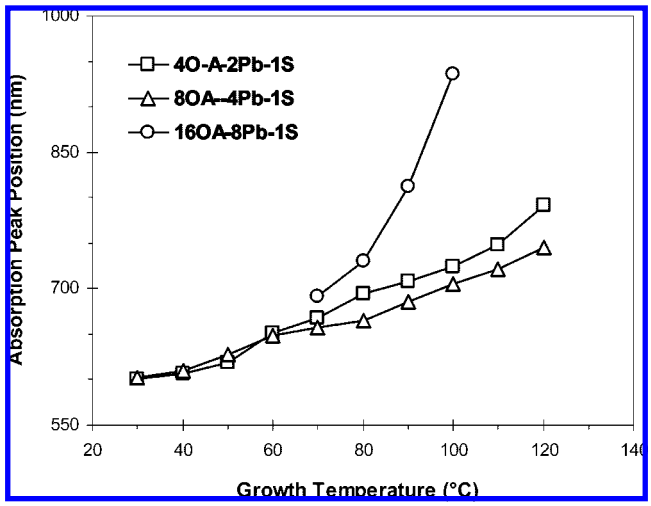

Figure 5. Comparison of the Pb-to-S feed molar ratios affecting the growth of PbS QDs with a fixed aicd-to-Pb feed molar ratio and S concentration under the synthetic conditions given in Table 1b. The absorption peak positions are presented by *y* axis in nanometers, while the growth temperature is on the *x* axis. The studied feed molar ratios are 4OA-2Pb-1S (□), 8OA-4Pb-1S (open triangular symbols Δ), and 16OA-8Pb-1S (○). No data is entered for the 16OA-8Pb-1S batch before 70 °C due to the lack of obvious absorption peaks leading to the ambiguous determination of the peak positions.

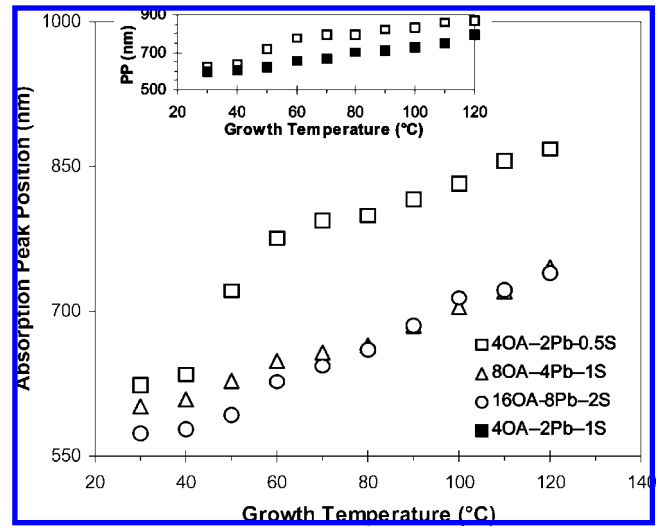

Figure 6. Comparison of S concentrations affecting the growth of PbS QDs with fixed 8OA-to-4PbO-to-1$(TMS)_2$S feed molar ratios under the synthetic conditions given in Table 1c. The absorption peak positions are presented by the *y* axis in nanometers, while the growth temperature is on the *x* axis. The studied S concentrations are 0.0175 M (4OA-2Pb-0.5S, □), 0.0350 M (8OA-4Pb-1S, Δ), and 0.0700 M (16OA-8Pb-2S, ○). The inset is to show the comparison of Pb-to-S feed molar ratios with a fixed acid-to-Pb molar ratio but different S concentrations; the two batches studied were with 4OA-2Pb-0.5S (□) and 4OA-2Pb-1S (■).

°C. A similar tendency, namely, large amount of acid leading to large nanocrystals, was observed in a hot-injection approach to CdS QDs; it was argued that the higher the acid concentration, the lower the CdS monomer reactivity, and the larger the CdS nanocrystals with broader size distribution formed.[26]

For the present noninjection approach to PbS QDs, the acid-to-Pb feed molar ratios have a strong influence on the formation of PbS QDs, and the amount of oleic acid plays an important role affecting the solubility of the resulting PbS QDs in the reaction medium. The larger amount OA, the larger the PbS nanocrystals, due to better reaction medium solubility.

3.1.1.b. Effect of PbO-to-(TMS)$_2$S Feed Molar Ratios with a 2OA-to-1PbO Fixed Feed Molar Ratio at 0.035 M Concentration of (TMS)$_2$S. After the investigation of the acid-to-Pb feed molar ratio with the typical synthetic procedure, the effect of the Pb-to-S feed molar ratio was also studied. Figure 5 shows the absorption peak positions of the growing PbS nanocrystals at different growth temperatures from three synthetic batches with the Pb-to-S feed molar ratios of 2:1, 4:1, and 8:1 at a fixed $(TMS)_2S$ concentration of 0.035 M and a fixed OA-to-Pb feed molar ratio of 2:1. Let us compare the two synthetic batches with 4OA-to-2PbO-to-1$(TMS)_2$S and 8OA-to-4PbO-to-1$(TMS)_2$S feed molar ratios: the former gave relatively large nanocrystals, as compared to the latter. As the Pb-to-S feed molar ratio increases, the peak positions of the bandgap absorption blueshift, indicating a decrease of the PbS nanocrystal size. A similar trend that large Cd-to-Se feed molar ratios favor small nanocrystals has been reported;[6g] it can be argued that high cation-to-anion feed molar ratios prevent the decomposition of already-formed PbS nanocrystals. In the case of 16OA-to-8PbO-to-1$(TMS)_2$S, the batch gave large nanocrystals due to the presence of large amount of acid. With a 1Pb-to-1S feed molar ratio approach, the nanocrystals grow too fast to exhibit well-defined bandgap absorption and emission, suggesting that the Pb-to-S feed molar ratio needs to be larger than 1:1 to avoid fast and uncontrollable growth.[6e]

3.1.1.c. Effect of Feed Concentrations with 2OA-to-1PbO and 4PbO-to-1(TMS)$_2$S Fixed Feed Molar Ratios. To understand the feed concentration, which can be simplified as S concentration, affecting the growth of nanocrystals, syntheses with different concentrations of the reaction agents with fixed OA-to-Pb-to-S feed molar ratios of 8-to-4-to-1 were conducted. There batches with the feed molar ratios of 4OA-2Pb-0.5S, 8OA-4Pb-1S, and 16OA-8Pb-2S were compared. Figure 6 shows the absorption peak positions of the resulting PbS nanocrystals at different growth temperatures from the three synthetic batches with the different feed concentrations. It is apparent that low concentrations gave large nanocrystals. S is the limiting reagent; when S concentration is low, it is relatively difficult for S to meet the Pb precursor leading to relatively big nuclei and nanocrystals with relatively broad size distribution.

Moreover, the inset in Figure 6 shows the absorption peak positions of the growing PbS nanocrystals at different growth temperatures from the synthetic batches with 4OA-2Pb-0.5S and 4OA-2Pb-1S feed molar ratios. Also, the 4OA-2Pb-0.5S batch gave relatively large nanocrystals. As we discussed before, large Pb-to-S feed molar ratios lead to small nanocrystals, while small S concentrations lead to large nanocrystals. Accordingly, when the effects of the Pb-to-S feed molar ratio and S concentration compete with each other on the particle size, the latter dictates, namely, it is the concentration rather that the Pb-to-S feed molar ratio dominants the growth of the nanocrystals under our experimental conditions.

On the basis of the investigation of the OA-to-PbO and PbO-to-$(TMS)_2$S feed molar ratios and reactant concentrations, an obvious conclusion can be drawn that these synthetic parameters affect the resulting PbS nanocrystal sizes, small OA-to-PbO and large PbO-to-$(TMS)_2$S feed molar ratios, together with high S concentrations favor small nanocrystals.

3.2. Effect of Acids as Capping Ligands. The previous work in our group has addressed the effect of the nature of capping ligands on the formation of magic-sized CdSe nanocrystals.[6g] It was observed that the chain length of fatty acids used affects on the activities of the Cd precursor and monomer; therefore, various acids were considered to synthesize PbS nanocrystals. With the

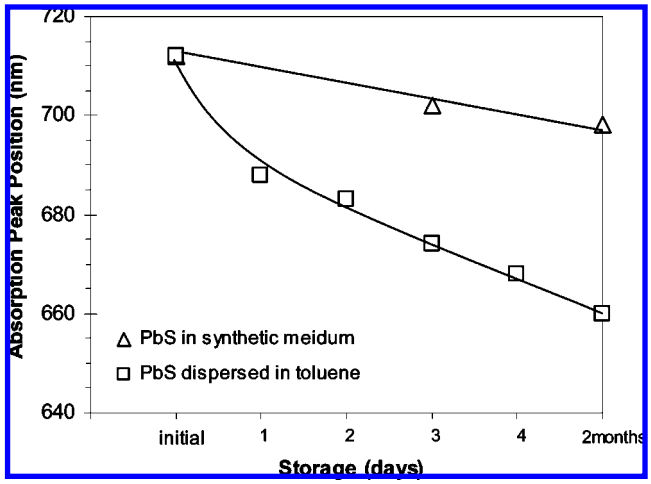

Figure 7. Storage stability monitored by the optical properties of the 70 °C growth PbS QDs (shown in Figure 1C-e). The ensemble was kept in toluene (□) and in synthetic medium (Δ). The absorption peak positions are presented by *y* axis in nanometers, while the storage periods are given on the *x* axis. The two solid lines are for eye guidance.

typical synthesis of the 4acid-to-2PbO-to-1$(TMS)_2S$ feed molar ratios, fatty acids with different carbon chain lengths ranging from C8−C24 were utilized as capping ligands instead of oleic acid. However, corresponding Pb carboxylate complexes formed at high temperature (120 °C) in ODE precipitated out at room temperature, with some even at 80 °C during the cooling process from 120 °C to room temperature; when the temperature was elevated again, the Pb-precursor precipitate dissolved and its solution became clear again. Thus, the solubility of the Pb carboxylate complex formed in ODE is good only at high temperatures (120 °C) and reduces along with the decrease of temperature. This phenomenon was also observed with oleic acid; but Pb oleate complex precipitates out only around 20 °C, which is lower than the reaction temperature, such as room temperature (30 °C). Accordingly, these fatty acids do not seem to be good candidates as capping ligands in the present synthetic system with our low-temperature and noninjection synthetic strategy, while oleic acid is.

3.3. Storage Stability of the As-Synthesized PbS Nanocrystals and Further Bandgap Engineering. In addition to the various synthetic parameters leading to high-quality PbS QDs, storage stability of the as-synthesized PbS QDs was also investigated to further evaluate the QD quality. Storage stability is an important parameter, regarding potential applications. Figure 7 shows the absorption peak positions of the 70 °C growth PbS nanocrystals (shown in Figure 1C-e) from the typical synthetic batch with the 4OA-to-2PbO-1$(TMS)_2S$ feed molar ratios before and after storage under ambient conditions and room light. The PbS QDs were stored in toluene (30 uL of QDs in 3 mL of solvent) and an in original synthetic environment. It is apparent that the storage medium influences the storage stability, regarding the degree of the blueshift of the bandgap absorption peak position: when this PbS ensemble was kept in a vial at room temperature under room light for days, less blueshift was observed than that dispersed in toluene and kept under the same condition. The blueshift of the absorption peaks may be attributed to the photo-oxidation of PbS particles.[27] The absorption and emission spectra are shown in Figure S5 of Supporting Information. It is noteworthy that, during the storage, no digestive/Ostawald ripening leading to self-focusing was observed, but the decrease in optical density and photoemission intensity was seen.

To promote the storage stability as well as further bandgap engineering after the formation of PbS QDs, PbS nanocrystals were

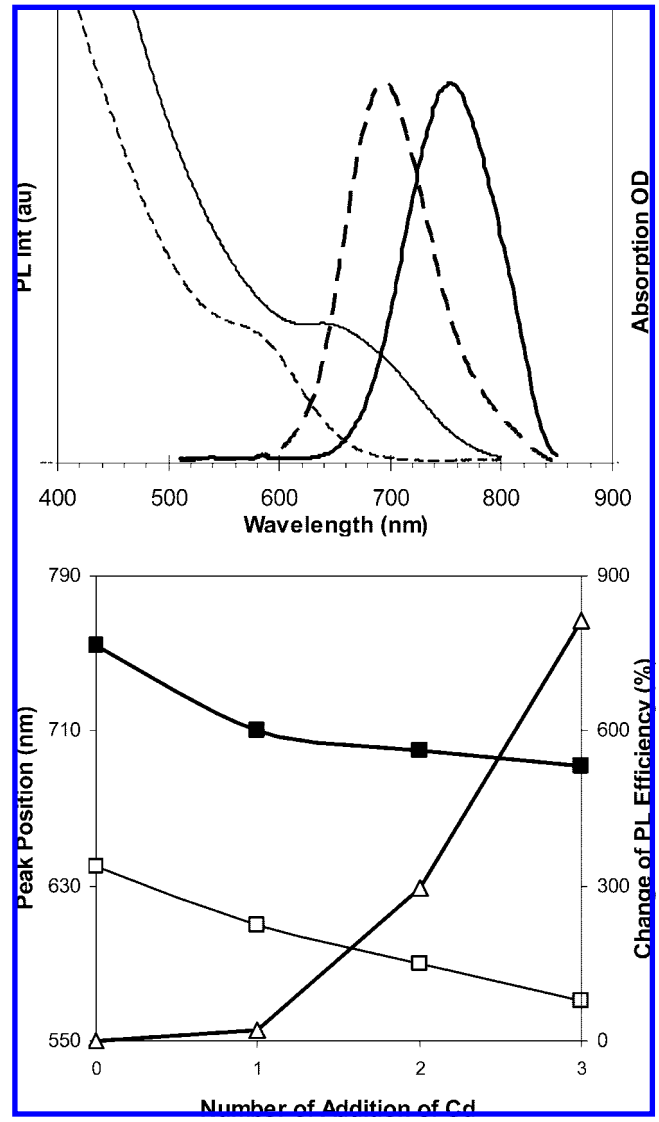

Figure 8. (Top) Absorption (thin lines, right *y* axis) and photoemission (thick lines, excited at 500 nm, left *y* axis) spectra of one as-synthesized PbS QD ensemble (solid line) and its corresponding PbS/CdS QDs (broken line). The PbS QDs were synthesized from a batch with feed molar ratios of 4OA-2Pb-1S and 20-min growth at room temperature. The post-treatment, namely, coating, was carried out at room temperature with a solution of Cd oleate in ODE. The QDs were dispersed in toluene and the spectra are normalized. (Bottom) The bandgap peak positions (PP, nm, left *y* axis) of the absorption (□) and emission (■) monitored before and after the post-treatment with the Cd oleate solution in ODE at room temperature together with the change of PL efficiency (right *y* axis) (open triangular symbols Δ). The *x* axis indicates the number of the addition of the Cd stock solution with the detailed synthesis given in Figure S6 of Supporting Information.

treated with a solution of Cd oleate in ODE at room temperature to obtain PbS/CdS nanocrystals exhibiting larger bandgap and higher emission efficiency. The top part of Figure 8 shows absorption and emission spectra of one PbS nanocrystal ensemble synthesized with 4OA-2Pb-1S feed molar ratios at room temperature and of its corresponding PbS/CdS nanocrystals prepared with the addition of a solution of Cd-oleate in ODE at room temperature. After the addition of Cd-oleate, the bandgap absorption of the resulting nanocrystals blueshifted from 640 to 571 nm, while emission shifted from 754 to 692 nm, shown in the bottom part of Figure 8. Also seen in the bottom part of Figure 8 is the blueshift of the bandgap absorption and emission peak positions during the addition of Cd-oleate, together with the increase of the PL efficiency, which was about 8 times. The blueshift and the increase

of the emission efficiency indicate that Cd replaced Pb on the QD surface leading to the formation PbS/CdS nanocrystals. It was reported that Cd ions replaced Pb ions in PbS nanocrystals resulting in a PbS/CdS core/shell structure; such ion-exchange coating was performed at elevated temperature 100 °C.[28] Here, our CdS coating was achieved at room temperature, which is facile, efficient, and green with energy saving. It is clear that the degree of the blueshift and the increase of the PL efficiency depend on the amount of Cd-oleate added. Accordingly, it is ready to further tune the optical properties of PbS nanocrystals synthesized through post-treatment at room temperature to obtain nanocrystals with larger bandgap and higher photoluminescence efficiency. TEM images of the QDs before and after coating are given in Figure S6 of the Supporting Information. After coating, the QDs exhibit less agglomeration. During coating, obvious color change was noticed and one example is shown in Figure S7 of the Supporting Information. Further study on coating with detailed characterization, such as X-ray powder diffraction, is being carried out in our laboratories. One example is presented in Figure S8 of the Supporting Information.

4. Conclusion

In summary, a noninjection and low-temperature approach to high-quality PbS QDs was developed, featuring easy handling and high reproducibility. This approach leads to small PbS QDs with bandgap in the range of 600−900 nm and narrow bandwidth. With one synthetic batch, it is possible to achieve various QD ensembles with tunable sizes controlled by different growth temperature, growth periods, acid-to-Pb feed molar ratios, feed reactant concentrations, and Pb-to-S feed molar ratios. Systematic investigation was performed on the synthetic parameters affecting the formation of PbS nanocrystals, including the various Pb and S source compounds. In general, various factors and the interplay between them play crucial roles leading to high-quality PbS QD products. Moreover, a ready post-treatment at room temperature with a Cd-oleate solution in ODE leads to CdS coating to achieve after-synthesis bandgap engineering with enhanced PL efficiency.

Acknowledgment. Tzuyu Liu thanks National Science Council of Taiwan for the financial support and the Science and Technology Division of the Taipei Economic and Cultural Office in Ottawa for assistance. Minjie Li thanks China Scholarship Council for the financial support and Chinese Ministry of Education in Ottawa for assistance. This work was supported by the National Research Council (NRC) of Canada, and Tzuyu Liu and Minjie Li thank the NRC International Relations Office.

Supporting Information Available: Comparison of non-injection and hot-injection approaches, comparison of S source compounds, comparison of Pb source compounds, comparison of the amount of acid, storage effect, TEM images of PbS and PbS/CdS, and pictures taken during a post-treatment with a solution of Cd oleate in ODE at room temperature. This information is available free of charge via the Internet at http://pubs.acs.org.

References and Notes

(1) (a) Michalet, X.; Pinaud, F. F.; Bentolila, L. A. J.; Tsay, M.; Doose, S.; Li, J. J.; Sundaresan, G.; Wu, A. M.; Gambhir, S. S.; Weiss, S. *Science* **2005**, *307*, 538. (b) Chan, W. C. W.; Nie, S. *Science* **1998**, *281*, 2016. (c) Liu, W.; Howarth, M.; Greytak, A. B.; Zheng, Y.; Nocera, D. G.; Ting, A. Y.; Bawendi, M. G. *J. Am. Chem. Soc.* **2008**, *130*, 1274. (d) Medintz, I. L.; Uyeda, H. T.; Goldman, E. R.; Mattoussi, H. *Nat. Mater.* **2005**, *4*, 435. (e) Lin, S.; Xie, X.; Patel, M. R.; Yang, Y.-H.; Li, Z.; Cao, F.; Gheysens, O.; Zhang, Y.; Gambhir, S. S.; Rao, J. H.; Wu, J. C. *BMC Biotechnology* **2007**, *7*, 67.

(2) (a) Song, H.; Lee, S. *Nanotechnology* **2007**, *18*, 255202. (b) Coe, S.; Woo, W.-K.; Bawendi, M. G.; Bulovic, V. *Nature* **2002**, *420*, 800. (c) Zhao, J.; Bardecker, J. A.; Munro, A. M.; Liu, M. S.; Niu, Y.; Ding, I.-K.; Luo, J.; Chen, B.; Jen, A. K.-Y.; Ginger, D. S. *Nano Lett.* **2006**, *6*, 463.

(3) Huynh, W. U.; Dittmer, J. J.; Alivisatos, A. P. *Science* **2002**, *295*, 2425.

(4) (a) Sargent, E. H. *Adv. Mater.* **2005**, *17*, 515. (b) Rogach, A. L.; Eychm″uller, A.; Hickey, S. G.; Kershaw, S. V. *Small* **2007**, *3*, 536. (c) Zhang, S.; Cyr, P. W.; McDonald, S. A.; Konstantatos, G.; Sargent, E. H. *Appl. Phys. Lett.* **2005**, *87*, 233101.

(5) Wise, F. W. *Acc. Chem. Res.* **2000**, *33*, 773.

(6) (a) Murray, C. B.; Norris, D. J.; Bawendi, M. G. *J. Am. Chem. Soc.* **1993**, *115*, 8706. (b) Peng, Z. A.; Peng, X. *J. Am. Chem. Soc.* **2001**, *123*, 183. (c) Manna, L.; Milliron, D. J.; Meisel, A.; Scher, E.; Alivisatos, A. P. *Nat. Mater.* **2003**, *2*, 382–385. (d) Yang, Y. A.; Wu, H.; Williams, K. R.; Cao, Y. C. *Angew. Chem., Int. Ed.* **2005**, *44*, 6712. (e) Yu, K.; Zaman, B.; Ripmeester, J. A. *J. Nanosci. Nanotech.* **2005**, *5*, 669. (f) Ouyang, J.; Ratcliffe, C. I.; Kingston, D.; Wilkinson, B.; Kuijper, J.; Wu, X.; Ripmeester, J. A.; Yu, K. *J. Phys. Chem. C* **2008**, *112*, 4908. (g) Ouyang, J.; Zaman, M. B.; Yan, F. J.; Johnston, D.; Li, G.; Wu, X.; Leek, D.; Ratcliffe, C. I.; Ripmeester, J. A.; Yu, K. *J. Phys. Chem. C* **2008**, *112*, 13805. (h) Nien, Y.-T.; Zaman, B.; Ouyang, J.; Chen, I.-G.; Hwang, C.-S.; Yu, K. *Mater. Lett.* **2008**, *62*, 4522. (i) Wang, R.; Ouyang, J.; Nikolaus, S.; Brestaz, L.; Zaman, Md. B.; Wu, X.; Leek, M. D.; Ratcliffe, C. I.; Yu, K. *Chem. Commun.* **2009**, DOI:10.1039/<B818967F> .

(7) (a) Sashchiuka, A.; Langofa, L.; Chaimb, R.; Lifshitza, E. *J. Cryst. Growth.* **2002**, *240*, 431. (b) Pietryga, J. M.; Schaller, R. D.; Werder, D.; Stewart, M. H.; Klimov, V. I.; Hollingsworth, J. A. *J. Am. Chem. Soc.* **2004**, *126*, 11752. (c) Zimmer, J. P.; Kim, S.-W.; Ohnishi, S.; Tanaka, E.; Frangioni, J. V.; Bawendi, M. G. *J. Am. Chem. Soc.* **2006**, *128*, 2526. (d) Baek, I. C.; Seok, S. I.; Pramanik, N. C.; Jana, S.; Lim, M. A.; Ahn, B. Y.; Lee, C. J.; Jeong, Y. J. *J. Colloid Interface Sci.* **2007**, *310*, 163.

(8) Dong, L.; Chu, Y.; Liu, Y.; Li, M.; Yang, F.; Li, L. *J. Colloid Interface Sci.* **2006**, *301*, 503.

(9) Zhao, P.; Chen, G.; Hu, Y.; He, X. L.; Wu, K.; Cheng, Y.; Huang, K. *J. Cryst. Growth.* **2007**, *303*, 632.

(10) Zhang, Y.-H.; Guo, L.; Yin, P.-G.; Zhang, R.; Zhang, Q.; Yang, S.-H. *Chem.−Eur. J.* **2007**, *13*, 2903.

(11) Wang, Z.; Zhao, B.; Zhang, F.; Mao, W.; Qian, G.; Fan, X. *Mater. Lett.* **2007**, *61*, 3733.

(12) Wang, W.; Li, Q.; Li, M.; Lin, H.; Hong, L. *J. Cryst. Growth.* **2007**, *299*, 17.

(13) Zhang, Y.; Chu, Y.; Yang, Y.; Dong, L.; Yang, F.; Liu, J. *Colloid Polym. Sci.* **2007**, *285*, 1061.

(14) Bakueva, L.; Gorelikov, I.; Musikhin, S.; Zhao, X. S.; Sargent, E. H.; Kumacheva, E. *Adv. Mater.* **2004**, *16*, 926.

(15) (a) Hines, M. A.; Scholes, G. D. *Adv. Mater.* **2003**, *15*, 1844. (b) Warner, J. H.; Thomsen, E.; Watt, A. R.; Heckenberg, N. R.; Rubinsztein-Dunlop, H. *Nanotechnology* **2005**, *16*, 175. (c) Abel, K. A.; Shan, J.; Boyer, J.-C.; Harris, F.; van Veggel, F. C. J. M. *Chem. Mater.* **2008**, *20*, 3794.

(16) (a) Cademartiri, L.; Bertolotti, J.; Sapienza, R.; Wiersma, D. S.; Freymann, G. V.; Ozin, G. A. *J. Phys. Chem. B* **2006**, *110*, 671. (b) Liu, J.; Yu, H.; Wu, Z.; Wang, W.; Peng, J.; Cao, Y. *Nanotechnology* **2008**, *19*, 345602.

(17) Nenadovic, M. T.; Comor, M. I.; Vasic, V.; Micic, O. I. *J. Phys. Chem.* **1990**, *94*, 6390.

(18) (a) Watt, A.; Rubinsztein-Dunlop, H.; Meredith, P. *Mater. Lett.* **2005**, *59*, 3033. (b) Patel, A. A.; Wu, F.; Zhang, J. Z.; Torres-Martinez, C. L.; Mehra, R. K.; Yang, Y.; Risbud, S. H. *J. Phys. Chem. B* **2000**, *104*, 11598.

(19) Yang, Y. J. *Mater. Sci. Eng., B* **2006**, *131*, 200.

(20) Zhong, M.; Wu, H.; Jiao, Z.; Li, Z.; Sun, Y. *Colloid. Surf. Physicochem. Eng. Aspect* **2008**, *353*, 13.

(21) Peterson, J. J.; Krauss, T. D. *Nano Lett.* **2006**, *6*, 510.

(22) Ferne′e, M. J.; Jensen, P.; Rubinsztein-Dunlop, H. *J. Phys. Chem. C* **2007**, *111*, 4984.

(23) Qiao, Z.-P.; Zhang, Y.; Zhou, L.-T.; Xire, Q. *Cryst. Growth Des.* **2007**, *7*, 2394.

(24) Ding, Y.; Liu, X.; Guo, R. *J. Cryst. Growth* **2007**, *307*, 145.

(25) Houtepen, A. J.; Koole, R.; Vanmaekelbergh, D.; Meeldijk, J.; Hickey, S. G. *J. Am. Chem. Soc.* **2006**, *128*, 6792.

(26) Yu, W. W.; Peng, X. *Angew. Chem., Int. Ed.* **2002**, *41*, 2368.

(27) Stouwdam, J. W.; Shan, J.; van Veggel, F. C. J. M.; Pattantyus-Abraham, A. G.; Young, J. F.; Raudsepp, M. *J. Phys. Chem. C* **2007**, *111*, 1086.

(28) Pietryga, J. M.; Werder, D. J.; Williams, D. J.; Casson, J. L.; Schaller, R. D.; Klimov, V. I.; Hollingsworth, J. A. *J. Am. Chem. Soc.* **2008**, *130*, 4879.

JP809171F